

High-Pressure Phase Transitions in AlPO_4 from First-Principles

WANG, Riping^{1*}, KANZAKI, Masami¹

¹ISEI, Okayama University

Based on first-principles density functional theory calculations, we predicted a ferroelastic transition in AlPO_4 between stishovite-like and $m\text{-CaCl}_2$ phases by confirming the energetic stability of stishovite-like phase and witnessing a pressure-induced phenomena of symmetry-breaking spontaneous strain, and furthermore, we established a new pressure-induced phase transition sequence for AlPO_4 up to 100 GPa at 0 K as follow: berlinite to moganite, to AlVO_4 , to $P2_1/c$, to CrVO_4 , to stishovite-like, and to $m\text{-CaCl}_2$ phase, with the corresponding transition pressure 4.1, 5.0, 7.0, 7.3, 31.9 and 46.4 GPa, respectively. For all these phases, equation of state parameters are reported. This transition sequence largely revises the previous one based on in-situ cold-compression experiments, by incorporating four new phases, moganite, AlVO_4 , the $P2_1/c$, and stishovite-like, the former three of which were synthesized by our recent quench experiments and are theoretically investigated here for the first time. This newly-established phase transition sequence would serve as a model case because it is the most detailed one among all the berlinite-type ABO_4 compounds to date. This study would also provide deep insight into the polymorphism behavior of SiO_2 because of some instructive dissimilarities discerned between these two isoelectronic compounds, such as that all the mixed-coordinated phases in AlPO_4 exceptionally lack counterparts in SiO_2 , and that moganite is stable after quartz phase in AlPO_4 but metastable in SiO_2 .

Keywords: AlPO_4 , SiO_2 , phase transitions, high-pressure, first-principles, equation of state

Prediction of NMR parameters by first-principles calculation: K-cymrite and polymorphs of AlPO_4

KANZAKI, Masami^{1*}, XUE, Xianyu¹

¹ISEI, Okayama Univ.

NMR spectroscopy is a powerful technique to study the local structure of solid materials. The interpretation of NMR spectra is greatly facilitated by the development of (1) advanced NMR techniques that provide direct through-bond and through space atomic connectivity information, and (2) first principles calculations of NMR parameters. For the latter, thanks to the development of periodic first-principles methods (Pickard & Mauri, 2001), the calculation of NMR parameters (chemical shift, and quadrupolar coupling constant and electric field gradient (EFG) asymmetry parameter for quadrupolar nuclei, such as ^{27}Al) from crystal structures has become feasible. In this study, we have applied this technique to calculate the NMR parameters for K-cymrite ($\text{KAlSi}_3\text{O}_8 \cdot \text{H}_2\text{O}$) that has a disordered Si/Al distribution and several AlPO_4 polymorphs, and have compared them with the experimental data.

NMR parameters were calculated using GIPAW method (Pickard & Mauri, 2001) implemented in Quantum-ESPRESSO (Giannozzi et al., 2009). For AlPO_4 -stishovite solid solution, a supercell of $2 \times 2 \times 2$ was used, and 2 Si were replaced with Al and P. For K-cymrite, a supercell of $2 \times 2 \times 1$ was used. Four different Al/Si disordered models were built.

For AlPO_4 , 5 polymorphs including three recently discovered high-pressure phases were calculated. Their crystal structures, ^{27}Al 3Q MAS and ^{31}P MAS NMR as well as other more advanced two-dimensional (2D) correlation NMR results have already been reported (Kanzaki et al., 2011; Kanzaki & Xue, 2012). The calculated chemical shifts of Al and P sites in these phases are within a few ppm from the observed ones. This further strengthened our previous site assignment of NMR peaks based on 2D correlation NMR experiments. We also calculated the chemical shift for P^{VI} in the SiO_2 - AlPO_4 stishovite solid solution. The calculated chemical shift for P^{VI} is about 105 ppm more negative than that of P^{IV} site in cristobalite. A recent experimental NMR study of 1 wt% AlPO_4 dissolved stishovite observed a peak about 130 ppm more negative than that of cristobalite, which was attributed to P^{VI} in stishovite (Stebbins et al., 2009). The general trend is consistent with our calculation, but there is a discrepancy of 25 ppm between the observed and calculated values. More detailed studies are necessary to resolve this discrepancy.

K-cymrite has a double-layered structure with Al/Si distributed in a single T site (Q^4). Our ^{29}Si MAS NMR revealed six peaks, although it has generally been assumed that a maximum of five peaks arising from different Si/Al distributions in the four next nearest T neighbors ($n\text{Si}$, $(4-n)\text{Al}$, with $n=0$ to 4) should occur for a single Q^4 site (Xue and Kanzaki, 2012). We have shown from direct 2D J-coupling mediated ^{29}Si NMR experiments that the $\text{Si}(3\text{Si}1\text{Al})$ and $\text{Si}(2\text{Si}2\text{Al})$ sites are each split into two peaks due to the existence of two populations of T-O-T angles (139° and 180°) (Xue and Kanzaki, 2012). In order to double-check this interpretation, the chemical shifts of $\text{Si}(4\text{Si})$, $\text{Si}(3\text{Si}1\text{Al})$ and $\text{Si}(2\text{Si}2\text{Al})$ sites were calculated for K-cymrite. The calculated chemical shifts of $\text{Si}(3\text{Si}1\text{Al})$ and $\text{Si}(2\text{Si}2\text{Al})$ sites show two distributions for each site separated by about 2 ppm, consistent with our experimental observation. The relative shifts between $\text{Si}(4\text{Si})$, $\text{Si}(3\text{Si}1\text{Al})$ and $\text{Si}(2\text{Si}2\text{Al})$ sites are also reproduced.

This study has thus demonstrated that first-principles calculation (GIPAW) of NMR parameters is a reliable mean to assist interpretation of NMR spectra for both ordered and disordered crystal structures.

References:

- Giannozzi, P et al. (2009) J. Phys: Condens. Matter, 21, 395502
- Kanzaki, M. and X. Xue (2012), Inorg. Chem., submitted
- Kanzaki, M. et al. (2011), Acta Cryst. B67, 30
- Pickard, C.J, and F. Mauri (2001), Phys. Rev. B., 63, 245101
- Stebbins, J.F. et al. (2009) Eur. J. Mineral., 21, 667
- Xue, X. and M. Kanzaki (2012), J. Phys. Chem. C., submitted

Keywords: NMR, first-principles calculation, chemical shift, crystal structure, AlPO_4 , K-cymrite

Determination of Transition Boundary between Garnet and Perovskite in CaGeO₃

ONO, Shigeaki^{1*}

¹JAMSTEC

It is known that some ABO₃ compounds are excellent analogues of MgSiO₃ or CaSiO₃, which are major constituents of the Earth's mantle. Calcium germanate (CaGeO₃) exhibits a sequence of phase transitions from a pyroxenoid to a tetragonal garnet phase, and subsequently to an orthorhombic perovskite phase. The phase boundaries in CaGeO₃ have been also used as a pressure calibration point at high temperatures in high-pressure experiments, such as for SiO₂ and Mg₂SiO₄. Therefore, the precise phase boundary of CaGeO₃ needs to be determined. The transition pressure of CaGeO₃ has been investigated in static high-pressure experiments using quench [1] and in situ methods [2]. According to previous high-pressure experiments, the transition pressure is ~6 GP and this boundary had a negative slope. In contrast, Ross et al. [1] also estimated the value of dP/dT slope of this transition using calorimetry data, and calculated the slope to be 2-3 times more negative than the value determined from high-pressure experiments. Therefore, we reinvestigated the dP/dT slope of garnet-perovskite transition in CaGeO₃ using the high-pressure experiments.

In this study, the use of a multi-anvil high-pressure system combined with a synchrotron radiation source made it possible to acquire precise data from samples under high-pressure and high-temperature conditions [3]. The starting material was CaGeO₃ wollastonite, synthesized at 1473 K for 5 hours from a starting mixture composed of finely powdered CaCO₃ and GeO₂. In our experiments, pressure was applied to the sample by generating an anvil load from the desired oil pressure in the press. The sample was then slowly heated to avoid the temperature overshoot until it reached the desired temperature for a given oil pressure. After reaching the required pressure and temperature, we performed in situ measurements using the synchrotron X-rays. The duration of heating was 0.5-2.0 hours. At the end of the experimental runs, the sample was quenched by cutting off the electrical power. This heating procedure was the same as that used in typical quench experiments.

We performed approximately 30 experimental runs, and the boundary determined in this study is in general agreement with that reported in previous high-pressure experiments [1,2]. However, the value of our dP/dT slope was 2-3 times more negative than that in previous experiments [3]. The calculated value of the dP/dT slope using calorimetry data [1] is consistent with our value of dP/dT [3]. It is likely that the discrepancy between previous and our high-pressure experiments is due to the kinetics of the structural phase transition. In previous in situ experiments [2], the P-T condition was changed several times during each run while observing the transition from the garnet to the perovskite structure. It is known that a metastable overshoot (pressure and/or temperature) is required to provide a sufficiently large energy driving force to overcome a nucleation and/or growth barrier for the transition in previous experiments [2]. To avoid any influence of the kinetic effect, we used the same heating cycle as that used in conventional quench experiments.

References

- [1] Ross et al. (1986) *J. Geophys. Res.*, 91, 4685-4696.
- [2] Susaki et al. (1985) *Geophys. Res. Lett.*, 12, 729-732.
- [3] Ono et al. (2011) *Phys. Chem. Minerals*, 38, 735-740.

Keywords: Garnet, Perovskite, Phase transformation, High pressure and high temperature

T-P-V equation of state of NaCl based on simultaneous measurements of elastic wave velocities and density of NaCl

MATSUI, Masanori^{1*}, Yoshihiro Okamoto¹, HIGO, Yuji², IRIFUNE, Tetsuo³, Ken-ichi Funakoshi²

¹Univ. Hyogo, ²JASRI, ³Ehime Univ.

The elastic compressional (P) and shear (S) wave velocities and densities of NaCl were simultaneously measured up to 12 GPa at 300 K, and up to 8 GPa at both 473 and 673 K, using a combination of ultrasonic interferometry, in situ synchrotron X-ray diffraction and radiographic techniques in a large-volume Kawai-type multi-anvil apparatus. We adopted experimental data after heating the sample to 873 K under fixed press loads, to minimize nonhydrostatic components due to local deviatoric stresses. At 300 K, both P and S wave velocities are found to change linearly with density up to 12 GPa, satisfying Birch's law. High-temperature and high-pressure equation of state (EOS) of NaCl was developed using the measured P and S wave velocities and densities based on the 300 K fourth-order Birch-Murnaghan finite strain equation combined with the Mie-Gruneisen relation and the Debye thermal model. Here we present a new temperature-pressure-volume EOS of NaCl, as a primary pressure standard, without relying on any pressure scale, at high temperatures and high pressures.

Keywords: high temperature and high pressure, elastic wave velocity, density, NaCl, equation of state

Sound velocity and structure measurement of silicate glasses under pressure

SAKAMAKI, Tatsuya^{1*}, KONO, Yoshio², WANG, Yanbin¹, PARK, Changyong², YU, Tony¹, JING, Zhicheng¹, SHEN, Guoyin²

¹GeoSoilEnviroCARS, Center for Advanced Radiation Sources, The University of Chicago, ²HPCAT, Geophysical Laboratory, Carnegie Institution of Washington

The degree of polymerization in silicate melt/glass is one of the most important parameters to understand the magma behavior. For silicate melts at ambient pressure, the degree of polymerization is highly related to composition, which is quantitatively described by a ratio of non-bridging oxygen (NBO) to tetrahedrally cation (T). In particular, the NBO/T is widely used to obtain viscosity information of various silicate melts and discuss the magma mobility in the Earth's interior. Several viscometry studies reported that polymerized melts showed much higher values of viscosity than those of depolymerized ones. Interestingly, it should be noted that the pressure dependence of the high viscosity of polymerized melts was shown to be negative. This gives important questions of the compression effect on the degree of polymerization and its effects on properties of silicate melts. In this study, we have measured the sound velocity of polymerized glass (jadeite and albite glass: NBO/T=0) and depolymerized glass (diopside glass: NBO/T=2) at pressures up to 10 GPa by using ultrasonic technique and synchrotron radiation with a Paris-Edinburgh press. We have also obtained the X-ray structure factor, $S(Q)$, of these glasses by using energy-dispersive X-ray diffraction method in order to understand structural changes in the intermediate-range order with pressure.

All experiments were conducted using a Paris-Edinburgh press, which is installed at the HPCAT 16-BM-B beamline, Advanced Photon Source (APS). High pressure sound velocity measurements were carried out using the ultrasonic pulse-echo-overlap method. The outer pressure media consisted of machinable zirconia pallets and sintered boron-epoxy. Graphite cylinder was used as a sample container, with a gold foil placed on top and bottom of the capsule as markers for sample length measurement. Radiography images taken by CCD camera allowed us to calculate the sample length under high pressure. Pressure was determined by the equation of state of gold, which was located below the sample. The scattered X-rays were detected using a Ge solid state detector (Ge-SSD) with a 4096 multi-channel analyzer. Alumina above the sample was used as a buffer rod. The glass sample and the alumina buffer rod were polished with 0.001 mm diamond paste. Ultrasonic signals were generated and received by a LiNbO₃ transducer. The signals were collected with a sampling rate of 5×10^9 point/second. Structure measurements were performed using the energy dispersive X-ray diffraction technique. The 16-BM-B is a bending magnet beamline which provides white X-rays (5-120 keV) with high brightness. The incident X-ray was collimated by two sets of vertical (0.1 mm) and horizontal (0.1 mm) slits. The diffracted signal was collimated with a 0.1 mm gap scattering slit 80 mm downstream from the sample and a 0.1 mm x 5.0 mm receiving slit 400 mm further downstream from the scattering slit. The Ge-SSD was mounted on a two-theta arm on a large Huber rotation stage, which allows accurate control on two-theta angle. The diffraction patterns were collected for 9 fixed diffraction angles ($2\theta = 3, 4, 5, 7, 9, 11, 15, 20, 25$ degrees). Collecting time varied with the diffraction angles, as intensities decreased with increasing angle. All patterns were collected until the maximum intensity reached at least 2000 counts. Structure factor, $S(Q)$, was obtained by combining X-ray diffraction profiles collected for 9 diffraction angles.

Pressure dependence of sound velocity of jadeite, albite and diopside glasses will be presented, along with structure factor $S(Q)$ of the glasses at high pressure. We would like to discuss a direct correlation between the intermediate-range order structure and sound velocity in these glasses, and the influence of the degree of polymerization.

Keywords: sound velocity, structure, glass, silicate, high pressure

Mapping of residual pressure around an inclusion in sapphire by fluorescence spectroscopy

KAMEGATA, Nanako^{1*}, NOGUCHI, Naoki¹, KAGI, Hiroyuki¹, Abduriyim Ahimadjan²

¹Geochemical Research Center, University of Tokyo, ²Gemological Institute of America

Residual pressure distributes around a mineral inclusion taken in a mantle-derived mineral represented by diamonds (e.g. Nasdala et al., 2003). It can provide useful information about the depth in the origin of the diamond by determining the residual pressure around a mineral inclusion in a diamond with spectrophotometric technique (e.g. Kagi et al., 2009). Differential stress between an inclusion and host mineral such as a diamond arises from differences in thermal expansion and compressibility between a mineral inclusion and host mineral. Corundum is the second hardest mineral and substantial residual pressure around an inclusion can be expected as well as diamond.

In general, corundum (Al_2O_3) includes a small amount of Cr^{3+} in the structure and fluorescence spectra attribute to Cr^{3+} ions can be obtained. Fluorescence spectra of corundum consist of R1 line at 694.3 nm and R2 line at 692.9 nm. The peak shift of the R1 line is affected by the differential stress, but the R2 line is not (Chai and Brown, 1996). So, we can estimate residual pressure from the peak position of the R2 line.

In this study, we used sapphire samples a kind of corundum. Around a mineral inclusion in sapphire, we measured fluorescence spectra using a three-dimensional fluorescence mapping system every 5 micrometers or 10 micrometers and determined residual pressure of each measurement point from the peak shift of the R2 line using a pressure calibration curve (Mao et al. 1986). We studied two kinds of sapphire samples; one is from Kings plains creek, Australia, and the other is from Kanchanaburi, Thailand. Albite, zircon and rutile were contained as mineral inclusion around 100 micrometer in size, and some of the inclusions have a radial crack. The maximum residual pressures around the zircon in the sample from Australia and albite in that from Thailand were determined to be 0.60GPa and 0.25 GPa, respectively. In the presentation, we will discuss the uptake process of the inclusion and the growth history of the sapphire from the pressure distribution around the inclusion.

Keywords: inclusion, sapphire, residual pressure, fluorescence spectroscopy

Experimental study on the phase transition of graphite to hexagonal diamond

OHFUJI, Hiroaki^{1*}, Tomoharu Yamashita¹

¹GRC, Ehime University

Hexagonal diamond (lonsdaleite) is a metastable polymorph of carbon and consists of ABAB... stacked sp³-bonded (tetrahedral) carbons. It occurs as microscopic crystals associated with graphite and cubic diamond in carbonaceous meteorites such as the Canyon Diablo meteorite and impact craters and can also be synthesized from well-crystalline graphite by high pressure experiments (e.g. Bundy and Kasper, 1967; Yagi et al., 1992). The phase transition of graphite to hexagonal diamond is considered to be a martensitic process, where [100] of hexagonal diamond is located parallel to [001] of the host graphite. However, we recently found a variety of such coaxial relations between graphite and hexagonal diamond based on TEM observations of samples synthesized by laser-heated diamond anvil cell (DAC). This suggests that the martensitic phase transition process is not always simple, but can be complex. Here, we conducted further research on the transition mechanism by using highly-oriented graphite samples with different crystallinities under different hydrostatic conditions.

We performed a series of high-pressure and high-temperature experiments at a pressure of 25 GPa and temperatures of 1800-2200K. Three types of highly-oriented graphite were used as starting materials: 1) highly-oriented graphite (HOG, Murakami et al, 1992), 2) highly-oriented pyrolytic graphite (HOPG) and 3) Kish graphite. Each sample was compressed in a DAC with/without an ethanol/methanol pressure transmitting medium and rapidly heated to a target temperature using fiber laser (1072 nm). The sample became transparent after laser heating, suggesting that the phase transition of graphite to diamond phase(s). The recovered samples were first examined by Raman spectroscopy for phase identification and then by transmission electron microscopy (TEM) for microtextural observations and electron diffraction analysis.

TEM observation revealed that the transparent area of recovered samples consists purely to mostly of hexagonal diamond with a layered structure similar to that of the graphite starting sample. A trace amount of cubic diamond also coexists in some cases. The electron diffraction (ED) patterns collected from pure hexagonal diamond synthesized from HOG and HOPG samples are complex and can be interpreted as a superposition of several types of reciprocal patterns in which [100], [002] and [-212] of hexagonal diamond are all arranged in a coaxial relation with graphite [001]. This suggests that the phase transition from graphite to hexagonal diamond proceeds mostly by $1/2(3a)^{1/2}$ or $1/(3a)^{1/2}$ shifts of graphene layers along graphite [100]. On the other hand, the ED patterns collected from Kish graphite are simple and can be indexed as a single reciprocal lattice where [100] of hexagonal diamond is parallel to [001] of the host graphite. It is likely that the crystallite size of hexagonal diamond synthesized correlates positively to the crystallite size (particularly in the a-axis direction) of initial graphite sources. Furthermore, the variety of the coaxial relation and transition process seems to be originated from the mosaicity (misorientation along c-axis) of the graphite sources.

Keywords: hexagonal diamond, graphite, laser-heated diamond anvil cell, TEM

Structural changes of silicagel by compression

MURAI, Takuro^{1*}, OKUNO, Masayuki¹, OKUDERA, Hiroki¹, ARASUNA, Akane¹, MIZUKAMI, Tomoyuki¹, ARAI, Shoji¹

¹Graduate school of Natural Science and Technology, Kanazawa university

The structural changes of silica gel by compression

Takuro Murai, Masayuki Okuno, Hiroki Okudera, Akane Arasuna, Tomoyuki Mizukami and Shoji Arai, Department of Earth Sciences, Kanazawa University, Kanazawa 920-1192, Japan

The structural change in amorphous silica gel ($\text{SiO}_2 \cdot n\text{H}_2\text{O}$) compressed up to about 1GPa and investigated by X-ray diffraction, Raman and Infrared spectroscopic measurements for elucidate the structural change processes.

Silica gel powder put in an Al alloy tube and compressed with 25kN to 200kN of press loads. Observed X-ray diffraction patterns show typical halo patterns for amorphous materials which have maxima at about $2\theta = 23^\circ$ (FSDP). FSDP shifted to higher angle by compression. Tan and Arndt (1999, J. Non-Cryst. Solids, 82, 117) reported that the shift of FSDP position to higher angle for compressed SiO_2 glass and this caused by decreasing in size of intermediate-range order of silica glass to increase its density.

In Raman spectrum, the 430 cm^{-1} broad band attributed to Si-O-Si symmetric stretching vibrations became sharp and the average position shifts to high wavenumber by compression. This shows that Si-O-Si angle in SiO_4 tetrahedral linkage in $\text{SiO}_4 \cdot \text{X}(\text{OH})_x$ decrease. The new band appears at 600 cm^{-1} in 50 kN and the intensity increase in increasing of compression load. This band has been attributed to three-membered rings of SiO_4 tetrahedra. The intensity of 980 cm^{-1} band of silanol groups increases by compression. This fact shows that some silanol groups reacts to dehydrate and form three-membered rings of SiO_4 tetrahedra. However, this dehydration reaction are limited and most H_2O and silanol groups were remained. Because, Raman band around 3500 cm^{-1} associate with H_2O almost remains its intensity after compression.

In IR spectra, the intensity of 800 cm^{-1} band of Si-O-Si bending mode increased by compression. It is consistent with formation of three-membered rings of SiO_4 tetrahedra those were found in Raman study. The FWHM of the 1080 cm^{-1} band increases and the band position shifts to lower wavenumber by compression. These facts show that the deformation of SiO_4 tetrahedron and the average Si-O length increase by compression.

Characterization of sulfur-containing calcite in a travertine carbonate rock

KIM, Hye-jin^{1*}, Jinwook Kim², Toshihiro Kogure¹

¹Department of Earth and Planetary Science, Graduate School of Science, the University of Tokyo, ²Department of Earth System Sciences, Yonsei University

Since the first documentation by Reeder and Wenk (1979), a number of studies reported weak extra reflections in rhombohedral carbonates in electron diffraction (ED) and referred to them as *c*-reflections. It was suggested that *c*-reflections are formed by the ordering of impurity cations such as Mg²⁺, Fe²⁺ and Mn²⁺ substituting Ca²⁺ (e.g. Reeder, 1981). Recently we have also found weak extra reflections similar to *c*-reflections in the ED patterns of calcite precipitated in a hot-spring (La Duke) near Yellow Stone National Park. The Selected-area ED pattern along the [001] direction indicated that the extra reflections appear holding the three-fold symmetry of calcite. Those weak reflections were found halfway between principal reflections. However, X-ray microanalysis indicated that the amount of impurity cations such as Mg²⁺ is very small and sulfur (S) is the major impurity element. S/Ca atomic ratio is about 3%. The cell parameters of the La Duke sample were determined by synchrotron X-ray powder diffraction (wavelength = 0.7749 angstrom) and Rietveld refinement. It showed that the *a*-length (4.9757 angstrom) slightly decreased and the *c*-length (17.0998 angstrom) slightly increased compared to the pure calcite (*a* = 4.9906 angstrom, *c* = 17.0621 angstrom), or the *c/a* axial length (3.437) of La Duke calcite is longer than that of pure calcite (3.419). The TG-DTA analysis was performed to find whether the sulfur exists in the calcite crystal or as organic matter. The anhydrite (CaSO₄) was detected at 600 degrees C and the *c*-length has recovered to that of pure calcite, suggesting that sulfur are incorporated in the calcite as a solid solution. XPS analysis was used to determine the chemical species of sulfur. Since the sulfur 2p_{3/2} peak of La Duke is located at 168.35 eV, the sulfur is involved in the ions of sulfate (SO₄²⁻). The crystal structure of La Duke calcite has been investigated using a four-circle X-ray diffractometer (Mo, wavelength = 0.71075 angstrom). Weak electron density around the oxygen was found, which may be related to the SO₄²⁻.

Keywords: calcite, electron diffraction, sulfur, superstructure, travertine

Dendritic magnetite spherules produced by fine particle heating / quenching experiments

ISOBE, Hiroshi^{1*}, GONDO, Takaaki¹

¹Grad. Sch. Sci. Tech., Kumamoto Univ.

Magnetite is a common accessory mineral in various rocks. Crystal shapes and habits of magnetite show diversity depending on crystallization conditions, especially cooling rate. Characteristic dendritic or skeletal magnetite crystals occur in quench rims of effusive rocks (e.g. Szramek et. al., 2010). The dendritic magnetite also occur in micrometeorites undergone quick heating and quenching at atmospheric entry (e.g. Genge, 2008, 2006, Toppani and Libourel, 2003).

In this study, we constructed a fine particle free fall apparatus in a high temperature furnace and carried out crystallization experiments with quick heating and quenching. In the experiments with volcanic ash particles, we found quite characteristic dendritic magnetite spherules. From the powdered meteorite, we got melted artificial micrometeorites (Gondo and Isobe, 2012).

Experiments were carried out in a vertical tube furnace with CO₂, H₂ and Ar mass flow controllers to control oxygen partial pressure and total gas flow rate. At the top of the furnace, a silica glass tube with an orifice with approximately 0.5mm in diameter was set to keep falling rate of particles. Particles were retrieved in an alumina crucible at the bottom of the furnace tube.

Terminal velocity of silicate particles with 100 micron meters in diameter in Ar gas at 1200 degree C is 18 cm/sec. Gas ascent rate at 1200 degree C is 11 cm/sec in the furnace tube when gas flow rate is approximately 1 l/min at standard condition. The falling speed of the particles with 100 micron meters in diameter, therefore, is reduced to approximately 7 cm/sec. When the highest temperature of the furnace set to 1520 degree C, the falling particles reach 1400 degree C within 2 seconds, keep above 1400 degree C more than 1 second, and are quenched within 1 second. For the fine particles with 100 micron meters in diameter, time scale of thermal equilibrium by radiation is within 1 second.

With this experimental apparatus, we carried out quick heating / quenching experiments of volcanic ash particles from Sakurajima volcano. The volcanic ash particles are sieved to 60 to 160 micron meters in diameter, and contain plagioclase, pyroxene, magnetite and groundmass glass in various proportions. Some particles contain quite high volume fraction of magnetite. After the experiments, more than half of the volcanic ash particles were well melted to show spherical shape. Groundmass glass and plagioclase particles formed clear glass spherules.

From particles with high volume fraction of magnetite, we can see quite characteristic texture in which dendritic magnetite cover almost whole surface of the spherule. Magnetite dendrite crystals with particular crystallographic direction to the spherule surface also occur. We discuss on dendritic magnetite texture with heating / quenching rate of fine particles.

Keywords: magnetite, dendritic crystal, quench texture, fine particles

The formation process of the oligoclases and ternary feldspars in the felsic gneiss from Mt. Riiser-Larsen in Napier Com

KODAMA, Yu^{1*}, MIYAKE, Akira¹

¹Kyoto Univ.

Mt. Riiser-Larsen, East Antarctica is the one component of the Napier Complex. The Napier Complex consists of granulite-facies metamorphic rocks formed by multiple thermal events, including Late-Archean ultrahigh temperature metamorphism (Harley and Black, 1997). Based on ternary feldspar solvus models, the bulk compositions of ternary feldspars in felsic gneiss from Mt. Riiser-Larsen yield the minimum of metamorphic temperatures ranging from 1000 to 1110°C (Hokada, 2001). TH97012006 (hereafter shortend to 12006) is the garnet-porphyroblast-bearing portion of a garnet-bearing felsic gneiss from Mt. Riiser Larsen. This sample is almost composed of oligoclase (An₂₉Ab₇₀Or₁; hereafter shortend to Olg), and anti to mesoperthitic ternary feldspar (hereafter shortend to TF) composed of Olg lamellae and orthoclase (An₂Ab₈Or₉₀; hereafter shortend to Or). The mode of occurrence and textures of Olg grains and TF grains are heterogeneous.

We observed the micro-textures of TF grains using by transmission electron microscope (TEM) and revealed the formation process of the common type of micro-textures of TF grains in 12006, (-901) exsolution lamellae of TF grains. But it became apparent that some micro-textures were not explained by (-901) exsolution lamellae and coexistence of Olg grains and TF grains was not explained.

In this study, some elemental analyses and cathodo luminescence (CL) observations on Olg grains and TF grains that have different exsolution lamellae in 12006 were carried out using by scanning electron microprobe (SEM) and wavelength-dispersive X-ray spectroscopy (WDX), and more detailed formation process of these feldspars in 12006 was suggested.

In this sample, Olg grains and TF grains are distributed heterogeneously. Hokada (2001) and Kodama (2010, Annual Meeting of Japan Association of Mineralogical Sciences) reported that no significant compositional difference was found between the chemical compositions of Olg grain and those of Olg lamellae in TF grains. However, K-rich Olg grains were found in this study. Significant differences in distribution of K and CL are observed between some Olg grains. Therefore, these Olg grains formed at different stages. This could result from the following process; First, K-free Olg grains and K-rich melt arose from Olg-rich protolith by partial melting caused by metamorphism. After that, during cooling process, K-rich Olg grains crystallized from melt.

On the other hand, TF grains that have An₂₃Ab₅₆Or₂₁ as bulk composition, and are composed of coarse Olg lamellae about 100 μm in width and TF lamellae-like textures that are composed of (-901) fine Olg lamellae and Or lamellae up to 10 μm in width (hereafter shortend to TF lamellae) were found. The TF lamellae are consistent with common TF grains in the orientation of Olg-Or boundaries and the bulk composition (TF lamellae: An₁₇Ab₄₃Or₄₀, common TF grains: An₂₁Ab₄₈Or₃₁). Therefore, these TF lamellae were formed by spinodal decomposition too. Orientation of boundaries of coarse Olg lamellae and Or lamellae is not consistent with (-901), and the scale of these TF lamellae almost correspond to coarse oligoclase lamellae. Therefore, these textures suggest that coarse Olg and TF lamellae decomposed at higher temperature, and after, fine Olg and Or lamellae decomposed from coarse TF lamellae by spinodal composition at lower temperature. However, the former decomposition is not explained by any decompositional process in current phase diagram. For more informations about these textures, the reexamination of phase relationships of An-Ab-Or system at high temperature is needed.

Keywords: ternary feldspar, exsolution texture

Measurements of the vacant sites in crystal structure of magnetite by Mossbauer spectroscopy

TOMITA, Chihiro^{1*}, SHINODA, Keiji¹, Yasuhiro Kobayashi²

¹Graduate school of Department of Geosciences, Faculty of Science, Osaka City University, ²Kyoto University Research Reactor Institute

Magnetite ($[\text{Fe}^{3+}][\text{Fe}^{3+} \text{Fe}^{2+}]\text{O}_4$) is a strongly magnetic oxide iron mineral. When magnetite undergoes low temperature oxidation, vacant sites are formed at octahedral sites, and magnetite changes to maghemite ($[\text{Fe}^{3+}][\text{Fe}^{3+} \text{Fe}^{2+}_{2/3}] \text{X}_{1/3} \text{O}_4$ (X shows vacant sites.)). Magnetite changes to maghemite with increasing vacant sites, so a degree of low temperature oxidation can be estimated from the vacant sites. According to Nishitani and Kono (1982), grain size controls the transformation of titanomagnetites. When the grain size of titanomagnetite is less than 1 micrometer, titanomagnetite transforms to titanomaghemite under low temperature heating. However, titanomagnetite larger than 1 micrometer breaks into Fe-rich titanomagnetite and Ti-rich ilmenite under low temperature heating. In this case, titanomagnetite suffers high temperature oxidation. Nishitani and Kono (1982) estimated the degree of low temperature oxidation of titanomaghemite by X-ray diffractometer and Curie temperature. Another method to estimate vacant sites is a Mossbauer spectroscopy. Mossbauer spectroscopy is a sensitive method to estimate degree of low temperature oxidation than X-ray diffraction.

In this study, we measured Mossbauer spectra of natural titanomagnetite of Oarai, Ibaragi Prefecture, and estimated vacant sites in titanomagnetite. Titanomagnetite samples of various grain diameter were heated at fixed time and temperature. After measuring those heated samples by X-ray diffractometer to distinguish low temperature oxidation samples from high temperature oxidation samples, Mossbauer spectra of samples which underwent low temperature oxidation were measured. The vacant sites in titanomagnetite is calculated from the results of Mossbauer spectra.

Natural magnetite has solid solution between Fe_3O_4 , Fe_2TiO_4 and FeAl_2O_4 . Ti^{4+} and Al^{3+} must be considered to estimate vacant site of titanomagnetite by Mossbauer spectra, because Ti^{4+} and Al^{3+} must be vacant for Mossbauer spectra. However, method of correction remains unsolved. Therefore, we considered a new correction method.

Keywords: Mossbauer spectroscopy, Magnetite, Titanomagnetite

High-pressure X-ray absorption measurement of FeS: K-edge absorption spectra of Fe

KONDO, Tadashi¹, FUJII, Atsuhiko^{1*}, Shigefumi matsumoto¹, KAZUNORI, Tanaka¹, Hironori Nakao², Yuichi Yamasaki²

¹Graduate school of science, Osaka University, ²KEK-IMSS

Iron sulfide (FeS) is important material to consider the cores of terrestrial planets such as Earth and Mars. FeS has been known to undergo several structural and electro-magnetic phase transformations with increasing with pressure and temperature. FeS takes a troilite structure (FeS I) and antiferromagnetic insulator ($T_N = 598$ K) at ambient condition, and it undergoes three pressure-induced transitions from FeS I to FeS II (orthorhombic MnP related structure) above 3.4 GPa and then to FeS III (monoclinic phase), and further transition to FeS VI reported recently above 36 GPa. The structural transition from FeS II to III is accompanied by a loss of magnetic ordering induced by high-spin to low-spin transition of Fe. In this study, we observed electronic state of Fe in high pressure by X-ray absorption near edge structure (XANES) experiment combined with diamond anvil cell (DAC), for understanding the relation between structural transition up to FeS VI and electronic transition.

X-ray absorption experiments under high pressure were performed at the BL-3A in KEK-PF, Tsukuba, Japan. We compressed powdered FeS sample with NaCl and measured X-ray energy dependence of absorption in the range of X-ray absorption near edge structure (7.0-7.2 keV) until 47 GPa. It was irradiated in three different beam diameters 0.1 mm, 0.3 mm and over 0.5 mm. We analyzed the difference of spectral patterns caused by change of structure and beam size. Absorption edges did not show a significant difference in each structure. But the pre-edge of absorption edge became sharp with structural transformation to high pressure phase.

Keywords: FeS, XANES

Measurements of Elastic Constants of Single-crystal Garnet by High Frequency Resonant Ultrasound Spectroscopy

ONO, Kenya^{1*}, YONEDA, Akira², YAMAZAKI, Daisuke², TOMIOKA, Naotaka², YOSHINO, Takashi², WATANABE, Tohru¹

¹Department of Earth Science, University of Toyama, ²Okayama University

Garnet is a major constituent mineral in the lower continental crust, upper mantle, and subducted slab. Gabbroic rock in slab transforms to denser eclogitic rock along with subduction. This larger density, which gives a negative buoyancy to slab, is attributed to the existence of garnet. The abundance of garnet is thus a key to understand the dynamics of subduction. Elastic property of garnet is critical to constrain its abundance in subducted slab from seismic observations. We thus have studied elastic constants of a single-crystal garnet using a resonance method.

We used a natural single-crystal garnet of composition Alm80Py16Sps4 (source unknown). It was selected in terms of the uniformity of crystallographic orientation examined by SEM-EBSD. The orientation of the single crystal was determined by the X-ray precession method. The crystal was shaped into a rectangular parallelepiped (0.890x0.690x0.440 mm³). Each face was polished flat (< 1 micrometer) in an orientation parallel or perpendicular to {100}. The density, which is calculated from the chemical composition analyzed with EPMA and the lattice parameter (a= 1.154(1) nm) measured by XRD, is 4.091(8) x 10³ kg/m³.

The resonance spectrum was obtained from 3 to 11 MHz by using a measurement system specially designed for such a small sample (Yoneda et al., 2007, JJAP). Elastic constants were determined by repeatedly comparing the obtained resonance spectrum with a theoretical one, which was calculated for trial values of elastic constants. C₁₁, C₁₂, and C₄₄ are determined to be 296.0, 111.2, and 94.4 (GPa), respectively. These are quite close to values previously reported for garnet single crystals with similar compositions. We will also report the temperature dependence of elastic constants in this presentation.

Keywords: elastic constant, resonance method, garnet, EBSD, SEM

Crystal structure refinement of ferrihydrite using atomic pair distribution function (PDF) method

KYONO, Atsushi^{1*}, NISHIMIYA, Yuki², Yutaro Yoshigami¹

¹Earth Evolution Sciences, Graduate School of Life and Environment Sciences, University of Tsukuba, ²Transmission Electron Microscopy Station, National Institute for Materials Science

Ferrihydrite is a short-range ordered nano-crystalline iron (III) oxyhydroxide that has been recognized to play an important role in iron cycling in environmental, biological, and geochemical processes. Despite intensive research for the two last decades, the exact atomic structure of ferrihydrite is not fully established and is still matter of debate. Atomic pair distribution function (PDF) analysis is a powerful technique to obtain structural information of nanoparticulate materials. Michel et al. (2007) have recently presented a structure for ferrihydrite that was determined using the PDF method and synchrotron X-ray scattering technique. In the study, the PDF analysis is used to investigate and compare the structure of 6-line ferrihydrite and dehydrated ferrihydrite with the results of Michel et al. (2007). Ferrihydrite was synthesized by the method of Schwertmann and Cornell (1991). TEM observations show that the particle size of the ferrihydrite is highly uniform with a size distribution between 3 nm and 5 nm. X-ray measurements were performed on a Rigaku RAXIS RAPID imaging plate area detector with sealed-tube X-ray source (Mo-K α radiation, $\lambda = 0.71073$ Å, graphite monochromated) operating at 50 kV and 40 mA. The X-ray total scattering data were collected up to $2\theta = 72.2$ degree that corresponds to the value of $Q_{\max} = 10.4$ Å⁻¹. The crystal structure of ferrihydrite was refined in space group P63mc, with $a = 5.974(2)$, $c = 9.130(2)$ Å, $V = 282.18$ Å³, spherical diameter = 2.09 (1) nm, and that of ferrihydrite heated was with $a = 5.924(1)$, $c = 9.130(2)$ Å, $V = 277.48$ Å³, spherical diameter = 2.002 (4) nm, respectively. The crystal structures are composed of edge-sharing FeO₆ octahedra and corner-sharing FeO₄ tetrahedra, which form a two-dimensional layer-like structure perpendicular to the c axis. The tetrahedra exhibit significantly distorted configuration such that three oxygen atoms are found at a distance of 1.96 Å and the other at 2.08 Å. The dehydration process causes a unit cell contraction accompanied by a shrinkage of the a lattice parameter. The release of water molecules enhances the bond length and angular distortions of the octahedra and tetrahedra in ferrihydrite.

Keywords: Ferrihydrite, Nano-mineral, Transmission electron microscope, Atomic pair distribution function (PDF) method, Crystal structure

Transformation mechanism of the sodalite-to-cancrinite phase transformation in oxalate-bearing solution

ECHIGO, Takuya^{1*}, Hirohisa Yamada¹, Tamura Kenji¹, Tohru Suzuki²

¹Functional Geomaterials Group, National Institute for Materials Science, ²Advanced Ceramics Group, National Institute for Materials Science

Cancrinite, $\text{Ca}_6\text{Ca}_2(\text{AlSiO}_4)_6(\text{CO}_3)_2(\text{H}_2\text{O})_2$, is one of feldspathoid minerals occurring in alkaline rocks. The crystal structure of cancrinite consists of three-dimensional aluminosilicate framework in which various cations (e.g., Na^+ , K^+ , Ca^{2+}) and anions (e.g., CO_3^{2-} , Cl^- , OH^- , SO_4^{2-} , NO_3^- , $\text{C}_2\text{O}_4^{2-}$) are occluded. Recently, Chukanov et al. (2010) reported a new cancrinite group mineral, kyanoxalite $[\text{Na}_7(\text{AlSiO}_4)_6(\text{C}_2\text{O}_4)_{0.5-1.0}(\text{H}_2\text{O})_5]$, from the Khibiny-Lovozero Alkaline Complex, Kola Peninsula, Russia. The authors mentioned that kyanoxalite was formed by hydrothermal alteration of sodalite $[\text{Na}_4(\text{AlSiO}_4)_3\text{Cl}]$, however, experimental evidence of the transformation of sodalite into cancrinite was not provided. In this study, we synthesize oxalate-bearing cancrinite and discuss the formation mechanism.

Keywords: Cancrinite, Sodalite, Oxalate

Pressure dependence of swelling state of Na-montmorillonite

SATOH, Takeshi^{1*}, KAWAMURA, Katsuyuki²

¹Tokyo Institute of Technology, ²Okayama University

It is known that montmorillonite clay minerals have the property of swelling with water molecules hydrated to interlayer cations. Clay minerals present on and under the Earth's surface, forming a card-house structure consisting of montmorillonite stacks, and they hold interlayer water and external pore water. The relative abundance of interlayer water and external pore water contributes the macro-scale material properties such as permeability and viscosity. Sample preparation is following. Bentonite sample used in this study is mined from Tsukinuno Mine, Yamagata Prefecture, and it is purified to obtain montmorillonite (Kunipia-F, Kunimine Industry Co., Ltd.). Na-montmorillonite, of which interlayer cation was replaced by sodium ion, is used in this study. Dry Na-montmorillonite and pure water with appropriate ratio were sealed in a sample tube. Water contents were measured after experiments. Water content is between 30 ~ 50 wt%, and they have properties between highly viscous fluid and solid. Relation between dry density, water content and swelling state is observed. At small water content (~30wt%), swelling state is a 2-layer hydration state, and a 3-layer hydration state at the large water content(~50%). At intermediate water contents, 2-layer and 3-layer hydration state coexist. Experimental procedure is following. Basal spacings of Na-montmorillonite is examined using in-situ X-ray diffraction methods. To obtain the temperature and pressure conditions near the earth's surface (a depth of up to 1 km) in the laboratory, the environment-control system was used for in-situ X-ray diffraction methods. The experiments were carried out to varying sample temperature from 30 to 80 degree at 10 MPa, and sample pressure from 10 MPa to 50 MPa at 30 degree. The exchange of water between interlayer and external pore was determined from swelling state change due to pressure and temperature. As a result, the swelling states, which is determined strongly by the water content or dry density, changes slightly due to pressure and temperature. By increasing temperature, there is a tendency that swelling state changes from 3-layer to 2-layer. Temperature dependence of swelling state is mainly on entropy. So, by increasing temperature, water moves from interlayer to external pore, which has higher entropy, and swelling state changes from 3-layer to 2-layer. Pressure dependence is mainly on molar volume, but there is almost no difference between the volume of interlayer water and external pore water. So, it is difficult to observe the pressure dependence. We are going to observe pressure dependence at higher than 50 MPa of swelling state.

Keywords: Montmorillonite, Smectite, Fault gouge, Radioactive waste

Molecular dynamics simulations of sodium tri-silicate melt under high pressure

NORITAKE, Fumiya^{1*}, KAWAMURA, Katsuyuki¹

¹Graduate school of environmental science, Okayama University

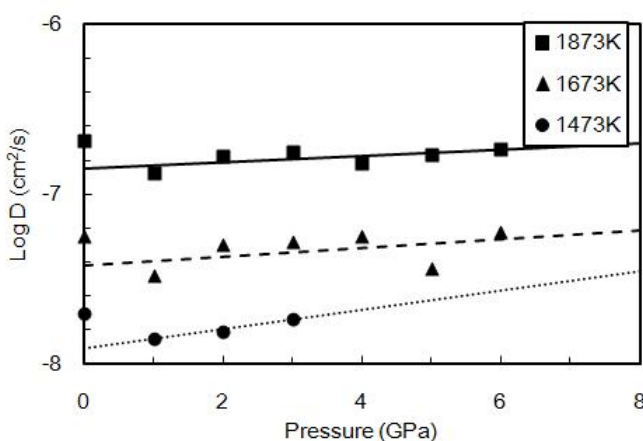
To understand volcanic process, genesis of magma, its ascent, and terrestrial magma ocean, the properties of silicate melts under high pressure must be investigated. The properties of silicate melts show peculiar behaviors under high pressures. It is reported that viscosity of acidic silicate melts decreases with increasing pressure (Scarfe et. al 1979). Moreover, it is reported that self diffusion coefficients of O and Si increases with increasing pressure (Rubie et al. 1993). These show that silicate melts soften under high pressure. In this work, the relationship between the structure and properties of $\text{Na}_2\text{O}_3\text{SiO}_2$ melt was investigated by molecular dynamics (MD) simulations. In MD simulations, it is possible to obtain changing configuration of every atom as a function of time. It is also possible it identify the individual atoms or groups of atoms which play a deciding role in diffusion processes.

MD simulations were performed with NPT ensemble ($N = 8002$) using MXDORTO. Pressure range is 0.1 MPa to 6 GPa (Every 1 GPa). Temperature range is 1473K to 2073K (Every 200K). Time step of equations of motion of atoms is 0.5 fs. The inter-atomic potential model implicitly includes Coulomb potential, short-range repulsion, van der Waals force and covalent terms. Starting from a random coordination and velocities, all the atoms are moved in Newtonian equation maintaining isobaric and isothermal through 2 ns as structural relaxation. After relaxation, statistical averages of physical properties were obtained through 200ps.

In 0 to 2 GPa, the density increases rapidly and Q^4 species increases with increasing pressure. This might means, the polymerization affect to the melt density in that pressure range. Shrinking of Si-O network is composed from increasing large membered rings and decreasing Si-O-Si angles. Small membered rings have small degree of freedom of deformation and large membered rings have large degree of freedom of deformation. Consequently, large membered rings might be easy to deform. In the MD simulations, the number of small membered rings decreases with increasing pressure and the number of large membered rings increases with increasing pressure. Adding to that, Si-O-Si angle decreases with increasing pressure. Consequently, this might be said that degree of freedom of deformation of Si-O network increases under high pressure and Si-O network is collapsed. Densification of $\text{Na}_2\text{O}_3\text{SiO}_2$ melt is occur as a result of that.

In MD simulation results, the self diffusion coefficient of oxygen decreases up to 1 GPa, then increases with increasing pressure. Using Einstein-Stokes relation, viscosity increases up to 1 GPa, then decreases with increasing pressure since self diffusion coefficient of oxygen controls the viscosity of silicate melts. The anomalous pressure dependence might be caused by distortion of Si-O network. One obvious structural distortion is decreasing of Si-O-Si angle. Si-O-Si angle become smaller than stable angle when Si-O-Si angle decreases under high pressure. And then, bridging oxygen becomes instable. Adding to that, distance between SiO_4 tetrahedra shorten. This structural change might activate diffusion of oxygen and SiO_4 tetrahedra. The other obvious structural distortion is decreasing of O-Si-O angle. The average O-Si-O angle decreases from the angle of regular tetrahedra with increasing pressure in MD simulations. Oxygen becomes instable when tetrahedra distorts because of repulsion between oxygen and distortion of sp^3 orbital.

Keywords: Molecular dynamics simulation, silicate melt, high pressure



Properties of water in rocks and minerals

FUKUDA, Jun-ichi^{1*}

¹Department of Earth Sciences, Graduate School of Science, Tohoku University

Water is ubiquitously distributed in the interior of the earth, forming various species. In rocks, water is trapped at intergranular regions as the form of H₂O fluid which are constructed by clustered H₂O molecules and as the form of -OH in mineral crystal structures. Also, in open cavities which are constructed by crystal structures, H₂O molecules are not clustered but isolated H₂O molecules are incorporated. It is well known that these water species contribute to earth dynamics such as reactions and deformation of minerals (recent studies of these subjects are summarized in Dysthe & Wogelius, 2006, Chem Geol). Based on these backgrounds, determinations of contents, distributions, states, migration rates, etc. are one of the most important subjects in earth sciences.

Infrared (IR) spectroscopy has widely been used to determine the above properties of water in rocks and minerals (See Aines & Rossman, 1984, JGR; Keppler & Smith, 2006, RIMG for IR spectra of various rocks and minerals). In this study, for advanced IR spectroscopic measurements, I will introduce high temperature in situ measurements and 2-dimensional mapping measurements based on my previous studies. First, I use chalcedonic quartz, which is constructed by microcrystalline quartz. Chalcedonic quartz contains abundant H₂O fluid at intergranular regions and mainly Si-OH in quartz crystal structures. Therefore, the properties of water are easily measured by IR spectroscopy. The sample is heated from room temperature up to 500 degree C, and changes of the states by temperature changes and dehydration will be discussed. Next, I use beryl, which contains isolated H₂O molecules in its open spaces of the crystal structure. Polarized IR spectra are measured at room temperature and high temperatures. Then, changes of the states of water will be compared with those of chalcedonic quartz. Finally, IR mapping measurements are performed for plastically-deformed granitoid (mylonite), and 2-dimensional distributions of water in polymineralic rocks are determined. Then, I will discuss relations of mineral phases, species and contents of water, in comparison with the results from the analyses of the states, diffusivity by dehydration as described above. I will also discuss possible microscale processes of water in relation to the deformation mechanism.

Keywords: H₂O, -OH, grain boundary, crystal structure, infrared spectroscopy

Effect of Al content and oxygen fugacity on water partitioning between olivine and orthopyroxene

SAKURAI, Moe^{1*}, TSUJINO, Noriyoshi¹, TAKAHASHI, Eiichi¹, KAWAMURA, Katsuyuki²

¹Department of Earth and Planetary Sciences, Tokyo Institute of Technology, ²Graduate School of Environmental Science, Okayama University

Water affects physical property of minerals (e.g. elemental diffusion rates, melting points). Because small amount of water plays key roles in mantle rheology, precise knowledge on partitioning of water among mantle minerals is very important in understanding the earth dynamics. Rauch and Keppeler (2002) investigated effect of Al content on water solubility in orthopyroxene. Al solubility of orthopyroxene decreases with increasing pressure above 3 GPa. Thus water partitioning coefficient may change significantly above 3 GPa. Moreover, Nishihara et al. (2008) indicated that substituting mechanism of OH in a mineral changes considerably with concentration of OH. Although water partitioning has been studied by many workers under water saturated conditions, experiments under low OH concentration are very limited.

In order to investigate the partitioning coefficient of water between olivine and orthopyroxene under low OH concentration (4~200 ppm), we performed high-temperature and high-pressure experiments using Kawai-type multi-anvil apparatus (SPI-1000) and piston-cylinder apparatus at the Magma Factory, Tokyo Institute of Technology, using starting materials of natural olivine (Ol; KLB-1) and synthetic orthopyroxene with various Al content (Opx; $(\text{Mg,Fe})_{2-x}\text{Al}_{2x}\text{Si}_{2-x}\text{O}_6$ ($x=0, 0.025, 0.05$)). Powdered minerals were enclosed in metal foil capsule (Ni, Mo) to form monomineralic layers with more than 300 micron meters in thickness each and put it in a $\text{Au}_{75}\text{Pd}_{25}$ capsule at pressures of 1, 3 GPa and temperature of 1300 °C. Oxygen fugacity was controlled by Ni-NiO and Mo-MoO₂ buffers. Water contents were obtained with a vacuum type Fourier transform infrared spectrometer (FT-IR6100, IRT5000). Water content of minerals was calculated based on Paterson's (1982) calibration. Run products were polished down to doubly polished slab. After polishing and prior to FT-IR analysis, samples were stored in a vacuum oven at ~120 °C over night. Detection limit in the IR spectra at 3200-4000 cm^{-1} is typically less than 1 ppm due to very low background of vacuum type FT-IR.

Water partitioning coefficient between Ol and Al free Opx are $D_{(\text{Al free Opx/Ol})} = 1\sim 2.3$. On the other hand, that between Al bearing Opx and Ol are $D_{(\text{Al bearing Opx/Ol})} > 4.1$. Thus $D_{(\text{Opx/Ol})}$ becomes larger with Al content of Opx. At constant temperatures, Al solubility of orthopyroxene stays nearly constant at ~3 GPa but becomes smaller with increasing pressure above ~3 GPa. Results of this study shows that amount of water in Opx is much larger than that in coexisting Ol below ~3 GPa. On the other hand, water content of Ol would become much larger than that of Opx above ~3 GPa. The IR spectra of Al bearing Opx show peaks broader than those of Al free Opx. Peak shapes of Al bearing Opx are similar to those of natural samples. The IR spectra of Ol in recovered samples under Ni-NiO buffer show additional OH band (3700 cm^{-1}) that are not seen in the spectra of run products under Mo-MoO₂ buffer. We are performing further high pressure experiments using Ol single crystal to avoid grain-boundary effects on adsorbing water.

Keywords: FT-IR, partitioning coefficient, upper mantle, olivine, orthopyroxene

Iron diffusion in mantle olivine under steep temperature gradient

YASUI, Toshinori^{1*}, KONDO, Tadashi¹

¹Graduate School of Science, Osaka Univ.

Laser-heated diamond anvil cell (LHDAC) has been generally used as a major method in which we can generate high temperature and pressure conditions of the Earth's interior. However, a strong temperature gradient is formed in the sample, because only a local region can be raised to high temperature by the laser heating technique. The Soret effect is known as a phenomenon of chemical diffusion induced by a temperature gradient, which causes a change of homogeneous material to heterogeneous chemistry. The Soret diffusion in liquids has popularly been studied and is fast, while that in solids and its pressure dependence have not been well examined because the Soret effect is relatively slow and more complex in solids than in liquids. Moreover, the investigation of Soret effect in solids under high temperature and pressure may be helpful to understand the possible diffusion in the Earth.

In this study, we studied the material experienced a steep temperature gradients using LHDAC and $(\text{Mg}_{0.89}\text{Fe}_{0.11})_2\text{SiO}_4$ San Carlos olivine as the starting material. The recovered samples were examined using a Field Emission-Scanning Electron Microscope (FE-SEM) and analyzed Mg-Fe interdiffusion. Chemical heterogeneity formation due to temperature gradient was observed in different experimental conditions such as temperature gradient, heating duration and phase transition. We will report the effect of these parameters on Soret diffusion in solid.

Keywords: LHDAC, Soret effect, diffusion in solid

Development of multi-axis DAC oscillation system for x-ray powder diffraction

YUSA, Hitoshi^{1*}, HIRAO Naohisa², OHISHI Yasuo², Mori Yoshihisa³

¹National Institute for Materials Science, ²Japan Synchrotron Radiation Research Institute, ³Okayama University of Science

Recent advanced experimental techniques of a laser-heated diamond anvil cell (DAC) provide wide P-T conditions in the earth's interior. Particularly, angular dispersive x-ray diffraction method combining with a high brilliance synchrotron radiation (SR) x-ray enables an access to the physical properties of the earth's constituent minerals. In this method, however, there is a significant quantitative problem to be solved. The spotty diffractions caused by coarse grains, which are likely generated during laser heating experiments, give an influence on the diffracted x-ray. In fact, the inhomogeneous x-ray profile leads to unreliable structure factors in Rietveld analyses. Thus, we hardly obtain ideal Debye rings being essential for the precise structural analyses due to the difficulty in acquiring sufficient particles satisfying Bragg condition. To improve this kind of statistical problem in the x-ray experiments using DAC, we have constructed the multi-axis oscillation system for x-ray powder diffraction measurements under high-pressure.

The oscillation system equipped a goniometer which was designed after the Gandolfi oscillation camera [1,2]. The goniometer has three oscillation axes, which are horizontal (theta), vertical swivel (omega), and rotating axes (phi) perpendicular to theta. The DAC with a large angular aperture (90 deg.), which is also newly developed for the oscillation system, is inserted into the holder on phi axis. The diffracted x-rays are detected with an imaging plate. This system has been installed in SR x-ray beam lines (BL04B2 or BL10XU) at SPring-8. In this presentation, we introduce details of the experimental set-up and a few experimental results using this system.

[1]G. Gandolfi, *Miner. Petrogr. Acta*, 13, 67-74 (1967)

[2]H.H. Otto, W. Hofmann, K. Schroder, *J. Appl. Cryst.*, 35, 13-16 (2002)

Keywords: high pressure, DAC, x-ray diffraction, Gandolfi camera, synchrotron radiation